Two degree of freedom motion control of an energy optimized aircraft ram air inlet actuator

N. Bajcinca, N. Schürmann, J. Bals

Institute of Robotics and Mechatronics
German Aerospace Center, DLR
82234 Oberpfaffenhofen, Germany

***Abstract*— A high accurate position control structure for energy optimal actuation of an aircraft ram air inlet actuator is presented in this paper. The structure comprises a feedforward planning of the energy optimal reference motion profile, and a feedback position control with an inner loop for speed tracking control using a robust two degree of freedom (inverse disturbance observer) controller. The motion control structure is validated by simulation and experimental results under different load conditions.**

I. Introduction

Due to various benefits, such as weight reduction, mounting costs and maintenance, the electro-mechanical technology is gaining more and more importance over the hydraulic one in aircraft actuation systems. An electromechanical ram air inlet actuator (RAIA) is used for the positioning of the air inlet of the heat exchanger of the air conditioning system of an aircraft cabin. The RAIA actuator typically operates at extreme thermal conditions with an overheating risk primarily due to actuation losses, thus giving impetus to investigation of energy optimized motion control.

This paper presents a position control structure, which includes a feedforward loop for the planning of optimal position and speed reference profiles, and a feedback loop for the position and speed control. The basic idea for the generation of reference profiles relies on the definition of the optimal actuation velocity v_o, as the speed at which for a given load the efficiency $\eta = P_m/P_e$ (P_m stands for the mechanical output power and P_e for the electrical input power) is maximal. However, it turns out that the amount of losses during the acceleration and deceleration phases are considerable, so the optimal profile planning must include these losses, too. In this paper the optimal speed profile is assumed to include an accelerated, a constant-speed and a decelerated phase.

The implementation of such a strategy needs a high accurate speed control loop. Therefore a novel two degree of freedom control structure referred as inverse disturbance observer is used. This structure is shown to provide good tracking behavior, in addition to robustness with respect to output disturbances and good sensitivity function responses within the operational bandwidth, [1].

The paper is organized as follows. Section II presents the testbed and the components of the RAIA actuation system. In Section III the generation of energy optimal motion profiles is briefly reviewed. Section IV focuses on the motion tracking control using the inverse disturbance observer controller. The simulation results and validation of the control strategy by experimental tests under compresion and traction load conditions are presented respectively in Section IV and Section V.

II. System description

The RAIA actuation system includes a single phase induction machine, a ball-screw spindle gear, a rotational and a linear speed sensor, as well as an electrical load actuator, see Fig 1. For operation in an aircraft the RAIA requires a 115 V/400 Hz supply voltage. The single phase induction machine is driven by exciting the main winding directly with the supply voltage and the auxiliary winding via a series capacitor used for 90° phase shifting. This delay is necessary for the production of a rotating field and a torque. In the non-transient operation the induction machine can operate with only the main winding. The roles of the two phases switch when the motor is driven in the opposite direction.

For the control of the RAIA a pulse width modulation (PWM) with 50 ms is used. This means that within one period of the PWM up to 20 sinusoids of the supply voltage pass thorugh the power electronic unit. The number of sinusoids is set by the input $0 \leq \alpha \leq 1$. For instance, $\alpha = 0.4$ lets 8 sinusoids pass through.

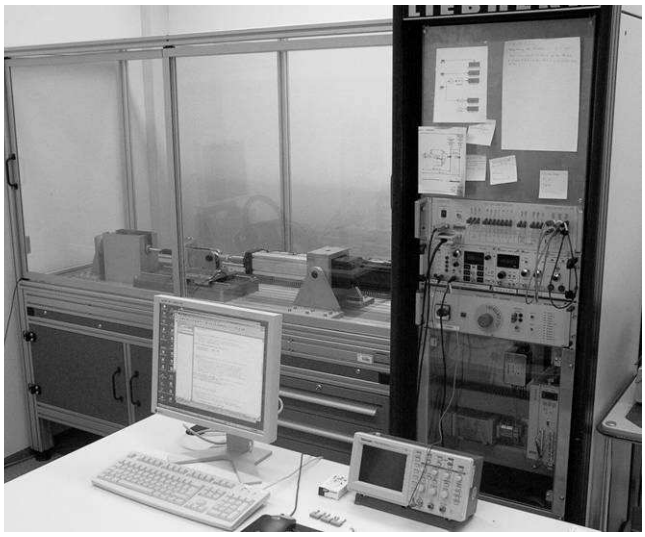

Fig. 1. The RAIA rapid prototyping test rig

The RAIA actuator is placed on a fixed bearing on the left side of the rapid-prototyping test rig, see Fig 1. A load actuator is used for the simulation of aerodynamic forces of the aircraft. The load actuator and RAIA are connected via a force sensor mounted on a plain bearing. Position control of RAIA and force control of the load actuaor are designed independently, whereby, of course, the load acts as a disturbance for the position control. Additional sensors are mounted for different investigations. For instance, the energy consumption of the RAIA is computed making use of current and voltage sensors. A temperature sensor placed on the surface of the RAIA is used for running experiments within a predefined temperature range. Finally, for dynamics modelling and identification purposes a high accurate position sensor is placed on the plain bearing.

III. Energy optimal actuation profiles

The structure of the energy optimal actuation of RAIA uses a feedforward stage for the generation of the energy optimal reference speed and position profiles for a given load. The basic planning strategy is driving the actuator as long as possible at the highest respective efficiency speed v_o. Therefore the optimal actuation is assumed to include three subsequent phases: (a) a constant-acceleration phase, (b) a constant-speed phase, and (c) a constant-deceleration phase. The optimal speed v_o is determined by experimental tests, that is, for a given load the actuator is driven at different constant speeds, whereby the actuation energy losses are computed. Note that the latter include mainly the electrical losses at the motor windings and the mechanical losses due to the gear friction. The obtained results for the compressive load are shown in Fig 2.

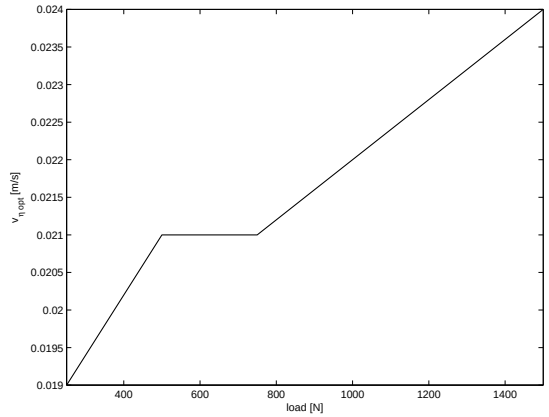

Fig. 2. Optimal efficiency speed for compressive load

The losses in the acceleration phase from zero speed to the optimal one v_o are also measured to conclude about the optimal acceleration a_o^+. The optimal deceleration a_o^- from v_o to $v = 0$ is determined similarly. The obtained results are shown in Fig 3. Given that a load uniquely defines v_o, a_o^+ and a_o^- are uniquely defined by that load, too. The dependency of the optimal acceleration and deceleration on the load are obviously quite different. With the increasing load the optimal

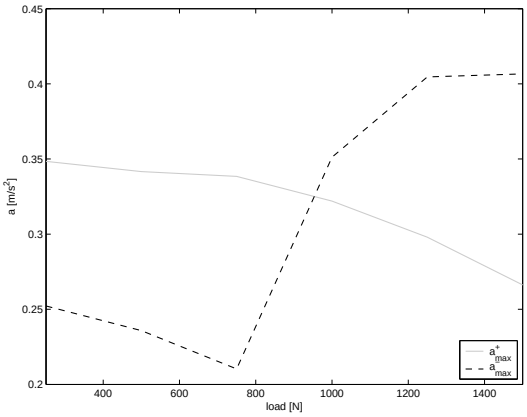

Fig. 3. Optimal acceleration and deceleration for compressive load (acceleration in gray)

acceleration decreases, while the optmal deceleration increases for the loads larger than 750 N.

IV. Control structure

The structure of the energy optimal actuation of RAIA is shown in Fig. 4. Last section discussed the feedforward stage 'Profile planning'. This section focuses on the feedback loop. The feedback stage is a standard structure cascading position and speed control loops. While for position control a proportional controller has been used, from the point of view of minimal energy actuation the accuratcy and robustness with respect to the load of the speed tracking loop is ultimative. Therefore a novel two degree-of-freedom controller, [1], has been used. This structure is briefly introduced in the sequel.

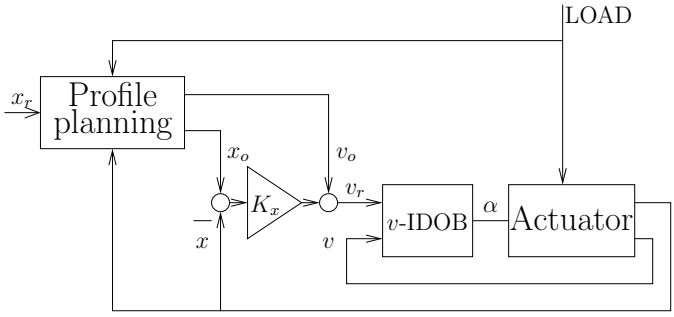

Fig. 4. Energy optimal control structure for RAIA

A. Two degree-of-freedom control structure

The structure of inverse disturbance observer (IDOB) controller is shown in Fig. 5. Basically it is a two-degree of freedom tracking control structure, which combines high-gain and exact model inversion control principles. The respective design parameters are a low-pass Q-filter and an approximate inverted model $\tilde{G}^{-1}$ of the plant G. The role of the feedforward controller $\tilde{G}^{-1}$ is provision of the main portion of the tracking control signal, which is further forced towards the exact tracking control output by the high-gain Q-loop. It can be shown that for $Q = 1/(\tau s+1)$ this statement holds exactly

for DC signals and approximately for frequencies within the bandwidth of Q. Notice that in the IDOB structure G is assumed to be minimum-phase and asymptotic stable.

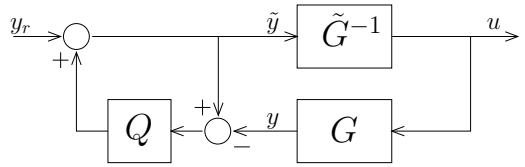

Fig. 5. Two degree-of-freedom inverse disturbance observer scheme

The transfer function from the desired output y_r to the output y in Fig. 5 is

$$\frac{y}{y_r} = \frac{G\tilde{G}^{-1}}{1 - Q(1 - G\tilde{G}^{-1})}. \tag{1}$$

For exact tracking $y = y_r$ has to be solved for the two degrees of freedom Q and $\tilde{G}^{-1}$. An intuitive and very simple solution which uses both degrees of freedom is

$$Q \approx 1 \quad \text{and} \quad \tilde{G}^{-1} \approx G^{-1}. \tag{2}$$

It is important to notice that principally both conditions on their own already solve the tracking problem. If $Q \approx 1$, then due to the positive feedback of the Q-loop in Fig. 5, a high-gain controller with infinity gain results. And, if $\tilde{G}^{-1} \approx G^{-1}$, then an exact feedforward inversion is realized and the feedback loop in Fig. 5 is idle. Therefore, the IDOB inversion structure unifies the high-gain and exact inversion principle.

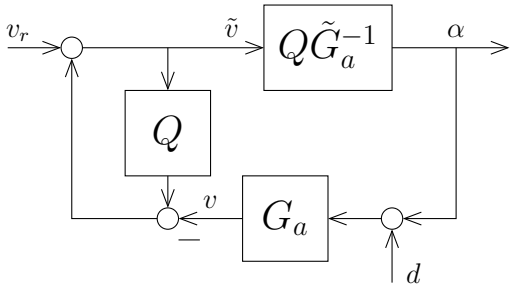

Fig. 6. IDOB scheme for speed tracking

B. Speed control

It has been shown that the input-output inherently nonlinear dynamics of a single phase induction machine is non-invertible, see [2] and references therein. Therefore applying the two degree of freedom structure therefore is related with the difficulty in a systematic design of $\tilde{G}^{-1}$. However, it can be shown that about an operating point in the speed-torque plane, the behavior of the single phase induction machine can be modelled by a linear first order system

$$\tilde{G}_a = \frac{K_v}{\tau_a s + 1} \tag{3}$$

where both parameters K_v and τ_a depend on the operating point. Here the input voltage of the actuator is a series of 400 Hz 115 V sinusoids which are switched on/off by a PWM

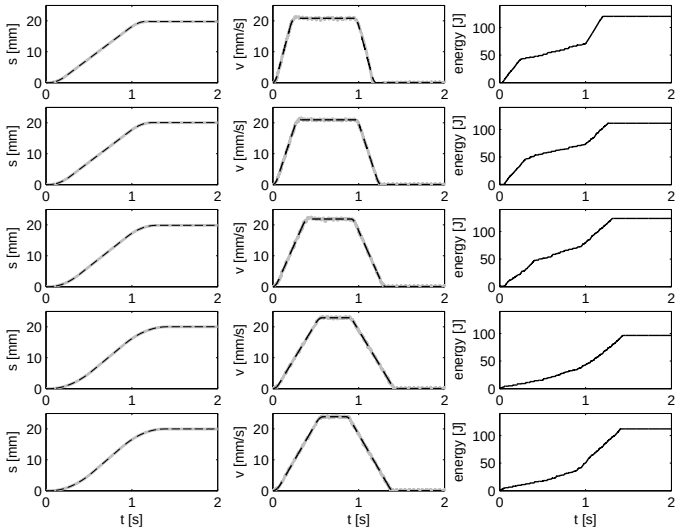

Fig. 7. Simulation results for energy optimized actuation with compressive load

module within 50 ms. The number of pulses is determined to the input α. To avoid acausalilty due to the improper inverse $\tilde{G}_a^{-1}$ the IDOB structure is modified as shown in Fig. 6. A Q filter of the first order

$$Q = \frac{1}{\tau s + 1}. \tag{4}$$

suffices to compensate the relative degree of $\tilde{G}_a^{-1}$.

Notice that the IDOB structure shown in Fig 6 is not identical to the basic one presented in Fig. 5. E.g. the input-output transfer function of causal IDOB reads

$$\frac{v}{v_r} = \frac{QG_a\tilde{G}_a^{-1}}{1 - Q(1 - G_a\tilde{G}_a^{-1})} \tag{5}$$

which is however still satisfying due to the high-bandwidth of the filter Q. Furthermore, the constant load modelled as an input disturbance d in Fig 6 is fully compensated since the sensitivity function

$$S = \frac{v}{d} = \frac{G_a(1 - Q)}{1 - Q(1 - G_a\tilde{G}_a^{-1})} \tag{6}$$

possesses a zero at $s = 0$, due to the condition $Q(0) = 1$.

C. Simulation results

Fig. 7 shows simulation results with the compressive loads 500 N, 750 N, 1000 N, 1250 N and 1500 N, respectively. In the first column are shown the reference and the measured position in [mm], in the second column the reference optimal speed v_o in [mm/s] and the measured one, and finally in the third one the actuation energy losses in [J]. The references are plotted dashed and the outputs in gray.

The IDOB controller is designed with $\tau = 0.001$ [s], $K_v = 35$ [mm/s] and $\tau_a = 0.06$ [s]. The simulation results show a high accurate tracking performance of the IDOB speed loop in all cases, independently on the load disturbance. Note that for higher loads the energy consumption increases, which is plausible.

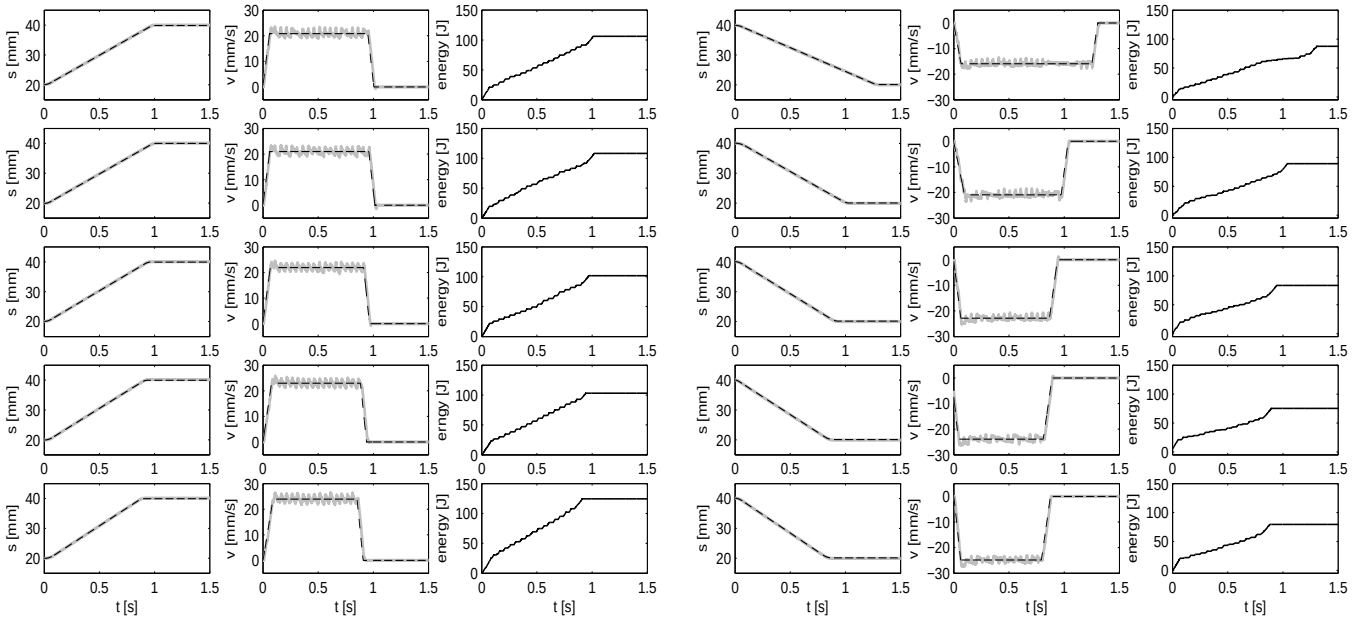

(a) Compressive load

(b) Tractive load

Fig. 8. Experimental results for energy optimized actuation

V. Experimental results

The obtained experimental results for the energy optimized actuation with inverse disturbance observer are shown in Fig. 8(a) and Fig. 8(b). The position trajectories in [mm] are plotted in the first, velocity in [mm/s] in the second and energy consumption in [J] in the third column. The reference trajectories for the position and the velocity are plotted in dashed lines while the measured trajectory is plotted in a solid gray line. Each row refers to a constant load beginning with 500 N and incrementing by 250 N up to 1500 N. Figure 8(a) shows the measurement with compressive and figure 8(b) with tractive force.

The agreement of simulation and experimental measurements is obvious from Fig 7 and Fig 8(a). From Fig IV-C it can be clearly seen that the energy consumption, as expected, under compressive conditions increases with the load. Under tractive load the opposite takes place. The latter is to be explained by the fact that the load actually may behave as a generator in this case. The stationary position error between reference value and actual value increases with the load, but its the maximum value is below 0.2 mm in all cases. Compared to a conventional feedback loop with PD control, the energy consumption is shown to be reduced up to 50%, [5], [6].

VI. Conclusion

This paper presents a control structure for the energy optimized actuation of an aircraft ram air-inlet actuator. It comprises a feedforward loop for the generation of the energy optimal reference motion profiles, and a feedback loop for speed and position control. The basic idea of the approach is to drive the actuator at the optimal efficiency speed as long as possible. Therefore a novel two degree-of-freedom control structure for robust tracking has been applied. The proposed control strategy is tested in simulations and experiments under different load conditions. In all cases a high accurate position and speed control has been achieved. It has been experimentally verified that such a strategy may provide power consumption up to 50% compared to a conventional PD feedback loop.

Acknowledgments

This project was granted by the Bavarian Department for Economy, Transportation and Technology under AZ300-3245.2-3/01. The authors would like to thank Liebherr-Aerospace, Lindenberg for their support during the project ”ECU (electronic control unit) test und optimization by hardware-in-the-loop simulations”.

References

[1] Bajcinca N., Bünte T.: “A novel control structure for dyanmics inversion and tracking”, *XVI IFAC Congress*, 2002 Prague.

[2] Bodson, M.: “Differential geometric methods for control of electric motors”, *International Journakl of robust and nonlinear control*, pp. 923-954, 1998.

[3] Dawson, D., H. Hu, T. Burg: “Nonlinear control of electric machinery”, *Marcel Dekker, Inc.*, New York, 1998.

[4] Mohan, N, T. Undeland, W. Robbins: “Power electronics”, *John Wiley, Inc.*, New York, 1995.

[5] Schürmann, N., Bals, J., Bajcinca, N. “Energieoptimale Regelung eines Ram-Air-Inlet Aktuators”, *Internal report*, Institut für Robotik und Mechatronik, DLR, Oberpfaffenhofen 2004.

[6] Bajcinca, N.,Bals, J.,Schürmann, N., Schweiger, C. “Test und Optimierung elektronischer Fahrzeug-Steuergeräte mit Hardware-in-the-Loop-Simulation”, *Final report 300-3245.2-3/01*, Institut für Robotik und Mechatronik, DLR, Oberpfaffenhofen 2004.

[7] Lehle, W. “Airbus A 330/340 environmental control system”, *SAE 24th International Conference on Environmental Systems and 5th European Symposium on Space Environmental Control Systems*, Friedrichshafen 1994.